Inorganic Chemistry

Communication

pubs.acs.org/IC

Synthesis and Crystallization Behavior of Surfactants with Hexamolybdate as the Polar Headgroup

Li Zhu,[†,‡] Kun Chen,[‡] Jian Hao,[‡] Zheyu Wei,[‡] Haocheng Zhang,[‡] Panchao Yin,*[,§] and Yongge Wei*[,‡,⊥]

[†]Beijing Union University, Beijing 100101, P. R. China

[‡]Department of Chemistry, Tsinghua University, Beijing 100084, P. R. China

[§]Chemical and Engineering Materials Division, Neutron Sciences Directorate, Oak Ridge National Laboratory, Oak Ridge, Tennessee 37831, United States

[⊥]State Key Laboratory of Natural and Biomimetic Drugs, Peking University, Beijing 100191, P. R. China

Supporting Information

ABSTRACT: Alkyl chains with different lengths were covalently grafted onto the surface of hexamolybdate through the postfunctionalization protocol of polyoxometalates. The obtained compounds represent typical structures of the so-called giant surfactants. Unexpectedly, those surfactants with hexamolybdates as polar headgroups are able to crystallize, while single-crystal X-ray diffraction reveals that the crystallization behavior of the surfactants is highly dependent on the length of the alkyl chains. For surfactants with comparatively short alkyl chains (C6 and C10), the alkyl chains prefer to interact with tetrabutylammonium, the countercation of hexamolybdate. However, the alkyl chains tend to pack with each other to form a domain of alkyl chains in the surfactant with a longer alkyl chain (C18). The possible mechanism is that a long alkyl chain cannot be fully compatible with the short chain (C4) of tetrabutylammonium.

Polyoxometalates (POMs) are a large group of well-defined molecular metal oxide clusters with sizes up to ∼6 nm.[1,2] Because of their outstanding and tunable acidic and redox properties, POMs have been demonstrated to be excellent catalysts for various reactions in both laboratory research and industry.[3−6] Very recently, POMs were also applied as electrochemical active materials for building batteries, supercapacitors, and memory devices.[7,8] The POM surface is fully covered by oxy, hydroxyl, or water ligands, making them completely hydrophilic, which significantly limits POMs' applications as catalysts because of their poor compatibility in organic media. In order to resolve the issue, the functionalization of POMs covalently/noncovalently with organic ligands was developed during the past decades.[9,10] The organic functionalization protocol provides a rational way to design and synthesize application-oriented POM−organic hybrids. Additionally, being different from pure inorganic POMs with high crystalline energy, the hybrids show the nature of soft matters, which renders us the ability to assemble them into functional materials with desired morphologies.[11−13] Especially, surfactants with POMs as the polar headgroup and surfactant-encapsulated POMs, as new classes of amphiphiles, have drawn increasing interest these years because of their rich and tunable solution behavior and potential applications as highly efficient emulsion catalysts.[11,14,15]

In recent years, a new class of amphiphiles called giant surfactants have been developed based on the functionalization of molecular clusters and nanoparticles.[11,16,17] Typical giant surfactants include, but are not limited to, the surfactants with POMs, fullerenes, POSS, and well-defined proteins as polar headgroups.[16] Different from the regular small-molecule surfactants, the giant surfactants possess unique and tunable phase behavior in both solid and solution states.[11,16,17] Noncovalent interactions, including van der Waals forces and hydrophobic, hydrogen-bonding, aromatic stacking, and electrostatic interactions, are responsible for the self-assembly process of giant surfactants and small-molecule counterparts.[11,16,17] However, rare studies have been carried out to investigate the exact interactions between the giant surfactants. Because of the disorders of the long surfactant tails, obtaining single crystals of these giant surfactants is challenging but helpful to characterize the molecular structure and details of specific noncovalent interactions among the giant surfactants.[15,18] Meanwhile, the single-crystal state of the giant surfactants could be beneficial in the applications of optic devices.[19,20] Herein, we report the synthesis and single-crystal structures of surfactants with hexamolybdate as the polar headgroup. The packing of the giant surfactants and their intercluster interactions are uncovered by single-crystal X-ray diffraction (XRD). Our work, to the best of our knowledge, reveals the significant role that the length of the alkyl tail plays in the formation of single crystals of the hybrid surfactants. The surfactants undergo a typical crystal-to-liquid crystal transition process when the temperature is gradually elevated.

Thanks to the significant progress that POM synthetic scientists have made during the last decades, the postfunctionalization of POMs and their hybrids has been well-developed, which renders us the ability to modify the POM surface with target functional groups.[9] We have successfully developed a protocol to introduce different ligands into hexamolybdate−organic hybrids through dicyclohexylcarbodiimide (DCC)-assisted esterification of the hexamolybdate-functionalized phenol, $(n\text{-}Bu_4N)_2[Mo_6O_{18}(NAr1)]$ (**1**; Ar1 = *p*-hydroxyl-*o*-

Received: April 22, 2015
Published: June 12, 2015

DOI: 10.1021/acs.inorgchem.5b00903
Inorg. Chem. 2015, 54, 6075−6077

toyl), with carboxylic acids.[21] Herein, long-chain *n*-alkylcarboxylic acids ($C_nH_{2n+1}COOH$, where n = 5, 9, 13, and 17) were first applied in the esterification reaction with compound **1**. Unfortunately, the desired surfactants with hexamolybdate as the polar headgroup can only be obtained in limited yields. However, while the corresponding long-chain carboxylic anhydrides were used to react with compound **1** in the presence of DCC in anhydrous acetonitrile, the hexamolybdate-headed surfactants, $(n\text{-}Bu_4N)_2[Mo_6O_{18}(NAr2)]$ (**2**−**5**; Ar2 = *p*-carboxylate-*o*-toyl), were obtained in good yields (Scheme 1). Significantly, their single crystals can be easily obtained via the slow diffusion of ethyl ether into the acetone solutions of the synthesized hybrid surfactants.

Scheme 1. Synthetic Reactions to Obtain Surfactants with Hexamolybdate as the Polar Headgroup

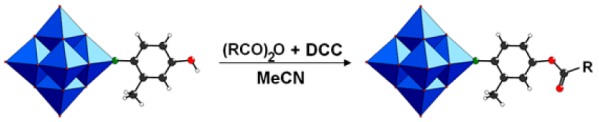

Single-crystal XRD, Fourier transform infrared (FT-IR), electrospray ionization mass spectrometry (ESI-MS), and UV−vis spectroscopic studies of compounds **2**−**5** confirm the structural features of both surfactants and hexamolybdate−organic hybrids (Figure 1). Single-crystal XRD results indicate

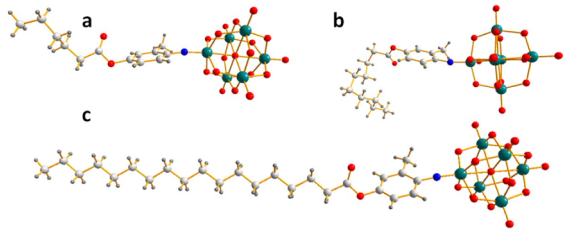

Figure 1. Ball-stick drawings of the molecular structures of the anionic surfactants with hexamolybdate as the polar headgroup: (a) compound **2**; (b) compound **3**; (c) compound **5**. Their counterions, TBA, are omitted for the sake of clarity.

that the hexamolybdate cluster framework remains intact while the organic fragments are covalently linked to the hexamolybdate cluster through a Mo≡N triple bond. The alkyl tails are covalently bonded to the phenyl ring via the ester group, confirming the success of the esterification reaction. The single-crystal XRD results are consistent with the FT-IR and UV−vis measurements of the corresponding samples. In the FT-IR spectra, characteristic peaks at 952 and 795 cm^{-1} are assigned as Mo═O and Mo−O−Mo vibrations, respectively, while a peak at 976 cm^{-1} is tentatively ascribed to the formation of a Mo≡N triple bond. The characteristic peak of the −OH vibration at 3412 cm^{-1} in the FT-IR results of hybrid **1** disappears, while new peaks at ca. 1760 cm^{-1} show up after the postmodification reaction, which is consistent with the formation of ester groups (see the Supporting Information, SI). The UV−vis spectra of compounds **1**−**5** indicate that there is a bathochromic shift of the lowest electronic transition from 325 nm of hexamolybdate to 365 nm of compound **1** and 354 nm of the hybrid surfactants. This shift results from the formation of a Mo≡N triple bond and the conjugation between the phenyl groups and the inorganic cluster. However, compared to compound **1**, there is an obvious blue shift in the hybrid surfactants due to replacement of the hydrogen atom of the phenolic hydroxyl group in compound **1** by the electron-withdrawing acyl groups during the esterification reaction. ESI-MS studies of the hybrid surfactants confirm the purity of these compounds and their stability in the solutions of acetonitrile for at least 1 week (Figures S2−S5 in the SI).

The lengths of the alkyl chains significantly affect the crystallization behavior of the hybrid surfactants. The single crystals of **2** and **3** show needle shape, while the single crystal of **5** shows 2D platelike morphology, implying the different packing styles between the hybrid surfactants **2**, **3**, and **5** (Figure 2). Both

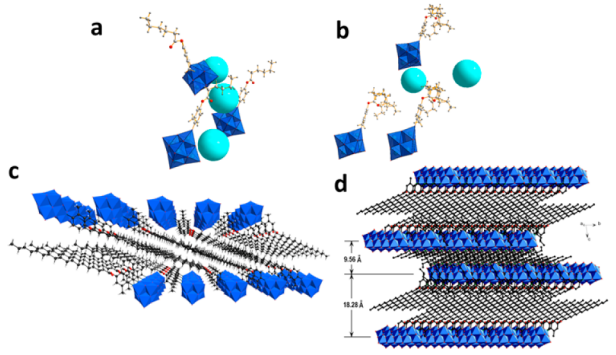

Figure 2. Graphical representation of the packing styles of the hybrid molecules in compounds **2** (a), **3** (b), and **5** (c and d): blue polyhedra, $Mo_6O_{18}N$ clusters; turquoise spheres, TBA cations.

compounds **2** and **3** crystallize in monoclinic space groups with similar cell parameters, suggesting the similar packing manner of the hybrid molecules in their crystals. However, compound **5** crystallizes in a triclinic space group (Table S1 in the SI). A further look at the detailed structure in the single crystals of all three compounds uncovers the reason for their different crystallization behaviors. In the single-crystal structures of **2** and **3**, the C6 and C10 alkyl chains grafted onto the surface of hexamolybdate collapse and interact with the tetrabutylammonium (TBA) cations that are associated around the neighboring hexamolybdate clusters. However, the hybrid surfactant molecules pack in a layer-by-layer manner in the single crystal of **5**. The alkyl chains are fully extended with a typical zigzag conformation in the single crystal of compound **5**. The alkyl chains, herein, prefer to interact with each other and form domains of close-packed alkyl chains which are sandwiched by two domains of POMs. Bridged by a layer of TBA, such POM−alkyl chain−POM layer structures with a thickness of 18.28 Å further pack to form crystals. The anisotropic interactions, as we describe above, in the crystal of compound **5** explain the formation mechanism of the 2D sheetlike crystals. Moreover, only the crystal of **5** among all of the hybrids studied in the work shows liquid-crystal behavior because of the different thermal behaviors of the inorganic POM domain and organic alkyl chain domain. Basically, at comparatively low temperatures, e.g., 45.84 and 80.86 °C, the alkyl chain domain will be melted, while the POM domain remains intact, resulting in the typical liquid-crystal behavior.

Lessons from small-molecule surfactants show that surfactants with long alkyl chains tend to crystallize with more difficulty and defects because of their great numbers of possible gauche conformations. Indeed, compared to the hybrid compounds **2** and **3**, compound **5** crystallizes much slower. However, the crystallization behavior of the hybrid surfactants is more complicated compared to their small-molecule counterparts

DOI: 10.1021/acs.inorgchem.5b00903
Inorg. Chem. 2015, 54, 6075−6077

mainly because of the existence of TBA, a countercation of the anionic surfactants. TBA, actually, is an amphiphilic cation that can interact not only with the C6 and C10 alkyl chains in compounds **2** and **3**, respectively, via its four hydrophobic tails but also with the POM polar headgroup through its positively charged nature. The case is different in compound **5** because the C18 alkyl chain is too long to be compatible with the four short chains of TBA. The C18 alkyl chains prefer to interact and pack with each other to form the alkyl chain domains.

On the other hand, the packing parameter, a widely applied concept that helps in the design of novel surfactants and predicts the self-assembly behavior of surfactants in the solution state, is also useful in understanding the crystallization behavior of hybrid surfactants. The crystallization and solution behavior of surfactants could be highly related because the packing of molecules plays a critical role in both of these different physical behaviors. The packing parameter (P) is defined in eq 1, whose value can be used to predict the formation of different types of assemblies (Table 1).[22] Nagarajan has thoroughly discussed the

Table 1. Packing Parameter Value and the Assemblies

P	assemblies in solution
$0 \le P \le {}^1/_3$	spherical micelle
${}^1/_3 < P \le {}^1/_2$	cylindrical micelle
${}^1/_2 < P \le 1$	bilayer
$1 < P$	reverse micelle

role that the tail length plays in P and the self-assembly process of the surfactants.[23] Generally, the packing parameter will be increased by elongating the tails. Therefore, it is expected that the P value increases from compound **2** to **5** when the length of tail was increased from C6 to C18 in our research. When P of the surfactants reaches ∼1, they prefer to form bilayer structures, which is consistent with the observed crystallization behavior of the four hybrid surfactants. Compound **5**, with the highest P value, crystallizes into a layer-by-layer structure, which represents a typical bilayer structure.

$$P = V_0/al_0 \quad (1)$$

where V_0 is the volume of the surfactant tail, l_0 is the length of the surfactant tail, and a is the surface area of the surfactant on the surface of the aggregates.

In summary, a series of surfactants with hexamolybdate as the polar headgroup were designed and synthesized for the purpose of studying their crystallization behaviors. As the first example of a comprehensive study of the crystallization behavior of POM–organic hybrid materials, our study uncovers the unique role that the lengths of alkyl tails play in the packing of hybrid surfactants. Our discovery should be instructive in the design of POM–organic hybrid crystalline and liquid-crystal functional materials.

■ ASSOCIATED CONTENT

Supporting Information

Experimental details, crystal information files (CIFs), and supportive figures. The Supporting Information is available free of charge on the ACS Publications website at DOI: 10.1021/acs.inorgchem.5b00903.

■ AUTHOR INFORMATION

Corresponding Authors

*E-mail: yinp@ornl.gov.

*E-mail: yonggewei@mail.tsinghua.edu.cn.

Notes

The authors declare no competing financial interest.

■ ACKNOWLEDGMENTS

We acknowledge the Clifford G. Shull Fellowship support from the Neutron Sciences Directorate at Oak Ridge National Laboratory, which is supported by the Office of Science of the U.S. Department of Energy under Contract DE-AC0500OR22725, and the support from the National Natural Science Foundation of China (NSFC Grants 21225103 and 21221062) and the Tsinghua University Initiative Foundation Research Program 20131089204.

■ REFERENCES

(1) Cronin, L.; Müller, A. *Chem. Soc. Rev.* **2012**, *41*, 7333.

(2) Long, D.-L.; Burkholder, E.; Cronin, L. *Chem. Soc. Rev.* **2007**, *36*, 105.

(3) Lv, H.; Geletii, Y. V.; Zhao, C.; Vickers, J. W.; Zhu, G.; Luo, Z.; Song, J.; Lian, T.; Musaev, D. G.; Hill, C. L. *Chem. Soc. Rev.* **2012**, *41*, 7572.

(4) Sugahara, K.; Satake, N.; Kamata, K.; Nakajima, T.; Mizuno, N. *Angew. Chem., Int. Ed.* **2014**, *53*, 13248.

(5) Sarma, B. B.; Neumann, R. *Nat. Commun.* **2014**, *5*.

(6) Rausch, B.; Symes, M. D.; Chisholm, G.; Cronin, L. *Science* **2014**, *345*, 1326.

(7) Miras, H. N.; Yan, J.; Long, D.-L.; Cronin, L. *Chem. Soc. Rev.* **2012**, *41*, 7403.

(8) Busche, C.; Vila-Nadal, L.; Yan, J.; Miras, H. N.; Long, D.-L.; Georgiev, V. P.; Asenov, A.; Pedersen, R. H.; Gadegaard, N.; Mirza, M. M.; Paul, D. J.; Poblet, J. M.; Cronin, L. *Nature* **2014**, *515*, 545.

(9) Proust, A.; Matt, B.; Villanneau, R.; Guillemot, G.; Gouzerh, P.; Izzet, G. *Chem. Soc. Rev.* **2012**, *41*, 7605.

(10) Dolbecq, A.; Dumas, E.; Mayer, C. d. R.; Mialane, P. *Chem. Rev.* **2010**, *110*, 6009.

(11) Yin, P.; Li, D.; Liu, T. *Chem. Soc. Rev.* **2012**, *41*, 7368.

(12) Yin, P.; Li, T.; Forgan, R. S.; Lydon, C.; Zuo, X.; Zheng, Z. N.; Lee, B.; Long, D.; Cronin, L.; Liu, T. *J. Am. Chem. Soc.* **2013**, *135*, 13425.

(13) Zhang, B.; Yin, P.; Haso, F.; Hu, L.; Liu, T. *J. Cluster Sci.* **2014**, *25*, 695.

(14) Yin, P.; Wang, J.; Xiao, Z.; Wu, P.; Wei, Y.; Liu, T. *Chem.—Eur. J.* **2012**, *18*, 9174.

(15) Yin, P.; Bayaguud, A.; Cheng, P.; Haso, F.; Hu, L.; Wang, J.; Vezenov, D.; Winans, R. E.; Hao, J.; Li, T.; Wei, Y.; Liu, T. *Chem.—Eur. J.* **2014**, *20*, 9589.

(16) Yu, X.; Li, Y.; Dong, X.-H.; Yue, K.; Lin, Z.; Feng, X.; Huang, M.; Zhang, W.-B.; Cheng, S. Z. D. *J. Polym. Sci., Part B: Polym. Phys.* **2014**, *52*, 1309.

(17) Li, D.; Yin, P.; Liu, T. *Dalton Trans.* **2012**, *41*, 2853.

(18) Yin, P.; Wu, P.; Xiao, Z.; Li, D.; Bitterlich, E.; Zhang, J.; Cheng, P.; Vezenov, D. V.; Liu, T.; Wei, Y. *Angew. Chem., Int. Ed.* **2011**, *50*, 2521.

(19) Liu, C.-G.; Guan, W.; Yan, L.-K.; Su, Z.-M.; Song, P.; Wang, E.-B. *J. Phys. Chem. C* **2009**, *113*, 19672.

(20) Hakouk, K.; Oms, O.; Dolbecq, A.; Marrot, J.; Saad, A.; Mialane, P.; El Bekkachi, H.; Jobic, S.; Deniard, P.; Dessapt, R. *J. Mater. Chem. C* **2014**, *2*, 1628.

(21) Zhu, L.; Zhu, Y.; Meng, X.; Hao, J.; Li, Q.; Wei, Y.; Lin, Y. *Chem.—Eur. J.* **2008**, *14*, 10923.

(22) Tanford, C. *The Hydrophobic Effect*; Wiley-Interscience: New York, 1973.

(23) Nagarajan, R. *Langmuir* **2002**, *18*, 31.

DOI: 10.1021/acs.inorgchem.5b00903
Inorg. Chem. 2015, 54, 6075–6077